Polarization splitter based on a square-lattice photonic-crystal fiber

Lorenzo Rosa, Federica Poli, Matteo Foroni, Annamaria Cucinotta, and Stefano Selleri

University of Parma, Parco Area delle Scienze 181/A, I-43100 Parma, Italy

A three-core polarization splitter based on a square-lattice photonic-crystal fiber is presented. The component separates the input field into two orthogonally polarized beams that are coupled to the horizontal and vertical output ports. The splitter has been designed through modal and beam propagation analysis by employing high-performance codes based on the finite-element method. Results obtained for a device length of 20 mm show extinction ratios as low as −23 dB with bandwidths as great as 90 nm. © 2006 Optical Society of America

OCIS codes: 060.2340, 230.1360, 230.5440.

Optical communication systems employ polarization splitters in many applications, such as coherent and polarization diversity optical detection.[1–3] In recent years the development of photonic crystals has allowed components to be devised to split the incoming light from a single-mode fiber into two orthogonally polarized beams coupled to two standard dielectric waveguides as well as allowed the study of devices based on photonic-crystal fibers (PCFs). PCFs are defined by a single bulk material containing a lattice of air holes running parallel to the axis, whose diameter and position can be chosen with great flexibility, allowing the construction of complex multicore structures. Good extinction ratios and short device lengths have been obtained by employing highly birefringent triangular-lattice PCF structures in a dual-core configuration[4,5] and, more recently, in a three-core configuration.[6,7]

These devices give rise to a couple of issues. First, the distance between the output cores is as small as 4 μm, less than the core diameter of a standard single-mode fiber, making it difficult to connect the device to its external outputs. However, a larger separation of the output cores substantially degrades coupling efficiency and overall splitting performance. The second issue is due to the triangular-lattice PCF itself when the structure has a central input core and two lateral output cores. To fit the lateral cores into the crystal, their distances and positioning from the central core have to follow the threefold symmetry of the lattice, resulting in asymmetrical positioning with respect to the polarization axes. Coupling behavior is thus different for the two polarizations, especially with respect to the coupling length.[7] Moreover, a birefringent core designed to couple one polarization cannot be adapted to the other by exchanging the axes, as it would not fit into a triangular lattice. Another core has to be designed with different hole diameters, thus increasing the structural complexity.

To overcome these drawbacks, a new polarization splitter has been proposed, based on a square-lattice PCF, which has recently drawn considerable attention for its interesting properties with respect to dispersion,[8] birefringence,[9] and cutoff.[10] The new device features a three-core directional coupler with a symmetric central input core and two highly birefringent output cores further than 20 μm apart. The device provides extinction ratios of about −23 dB over bandwidths as great as 90 nm, the extinction ratio being, for each output core, the power ratio of the undesired and the desired polarization. The design has been implemented by using a finite-element method (FEM) full-vector modal solver to properly draw the birefringent cores and by using a FEM-based beam propagation method (BPM) to evaluate the device length, which yields about 20 mm.

The new device is based on a square-lattice PCF whose parameters are $\Lambda = 4$ μm and $d/\Lambda = 0.4$, where d is the hole diameter and Λ is the lattice pitch. The splitter cross section is depicted in Fig. 1, where the input core is indicated as A and the output cores as B and C. The diameter of an unperturbed core, obtained by removing one hole from the lattice, can be assumed to be $\Lambda(2 - d/\Lambda) = 6.4$ μm. The high value of Λ achieves a large separation between the output cores and a wide input core. Moreover, it should be noted that the holes surrounding input core A, marked 1 in Fig. 1, have been modified to a diameter of 1.58 μm, preserving the twofold symmetry of the lattice, so that the core remains nonbirefringent. These two key design features reduce power loss due to modal mismatch at the junction between the
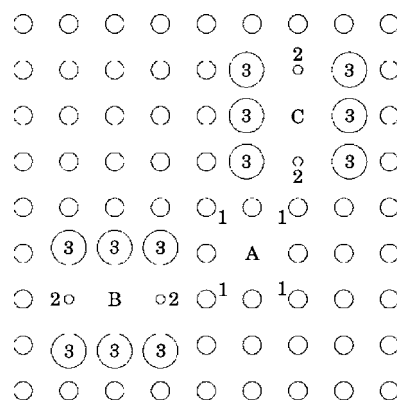

Fig. 1. PCF cross section of the square-lattice splitter. Parameters of the lattice are $\Lambda = 4$ μm and $d/\Lambda = 0.4$. Holes marked 1, 2, and 3 have d/Λ equal to 0.395, 0.2, and 0.755, respectively.
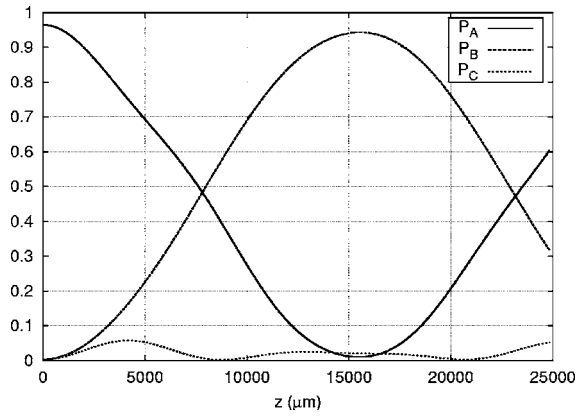
Fig. 2.   Normalized power evolution as a function of the splitter length z, considering an x-polarized input field. P_A, P_B, and P_C are the power curves evaluated for cores A, B, and C, respectively.
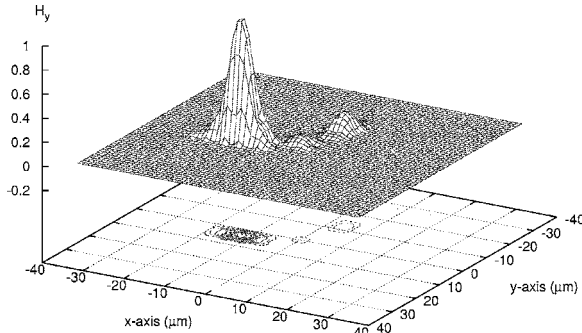

Fig. 3.   Dominant magnetic field component of the x-polarized field after a 15.7 mm propagation in the device.

single-mode fiber and the PCF. Instead cores B and C are surrounded by holes of different dimensions, marked 2 and 3 in Fig. 1, and having diameters of 0.80 and 3.02 μm, respectively. The asymmetry induces a strong birefringence, so that the effective indices of the two orthogonal polarizations are different.

The effect is exploited to achieve selective coupling of each polarization into a different output core by matching the desired effective indices. In particular, core B is designed to couple the horizontal x polarization and core C to couple the vertical y polarization. To this end, the FEM-based modal solver has been applied to core B by tuning the dimension of the holes marked 2 and 3 until the effective index for the x polarization, n_{Bx}, has achieved a value as close as possible to the corresponding one in core A, n_{Ax}. In the present design, their difference is $|n_{Ax}-n_{Bx}|$ $=1.09\times10^{-6}$ at the operating wavelength λ $=1.55$ μm. In contrast, the effective index difference for the two polarizations propagating in core B is $|n_{Bx}-n_{By}|=1.84\times10^{-4}$, 2 orders of magnitude higher. This ensures that the x-polarized modes of cores A and B will be strongly coupled, while the coupling between the y-polarized modes will be much weaker. The design of core C is simple, as it is derived from core B by exchanging the axes. Its features mirror those of core B, yielding $|n_{Ay}-n_{Cy}|=1.13\times10^{-6}$ and

$|n_{Cx}-n_{Cy}|=1.84\times10^{-4}$. The birefringent core positions in the PCF cross section and their distance from the input core have been chosen to allow power exchange. This is done by simulating the device by means of the FEM-BPM and fixing the reciprocal core position that provides maximum coupling.

Note that the effective indices of the various modes are influenced by the presence of the adjacent cores. This means that a further step has to be performed to reshape the birefringent cores in order to get the effective index differences previously reported. However, since the lattice cell is square, cores B and C can be positioned symmetrically with respect to the central core, preventing the induction of birefringence in the input core and keeping the effective index difference at a very low value of $|n_{Ax}-n_{Ay}|=5.6\times10^{-7}$. It should be noted that the final structure depicted in Fig. 1 yields a center-to-center distance between the two output cores B and C equal to 22.62 μm. The final hole distribution has a low number of different holes and is compatible with current fabrication technology, which is by now producing PCFs with submicrometer hole diameters.[11] Moreover, the required accuracy in the hole diameters must be guaranteed for just a few millimeters, as will be shown below.

It is finally important to emphasize that the designed cores allow very low coupling losses. In fact, at $\lambda=1.55$ μm, the effective area of the field in the input core is about 33 μm^2, which results in 0.8 dB losses when coupled with an 80 μm^2 effective-area single-mode fiber. Similarly, the effective area of the field in the output birefringent cores is about 34 μm^2, which results in 0.15 dB losses when coupled with a 49 μm^2 effective area bow tie polarization-maintaining fiber.

The power evolution analysis along the splitter confirms the design's correctness. As shown in Fig. 2, when an x-polarized field is fed into core A, the main part of the input power P_A is coupled into core B, as shown by the P_B curve, while there is little coupling into core C, as depicted by the P_C curve. On the other hand, when the input is y polarized the behavior is mirrored, providing the same graph as in Fig. 2 except for the P_B and the P_C curves, which are exchanged. Thus the power is split mainly into core C. The curves are normalized to the highest value of the input power and are obtained by integrating the field on rectangular subdomains enclosing the holes immediately surrounding each core. The coupling fea-
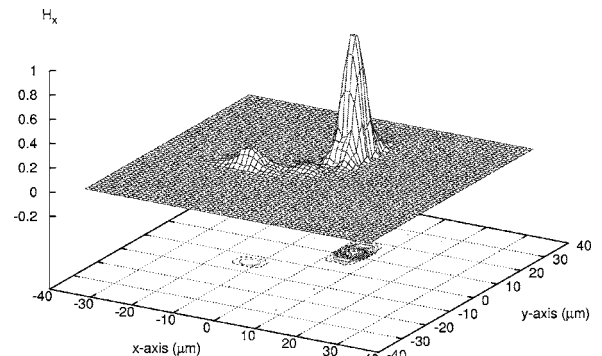

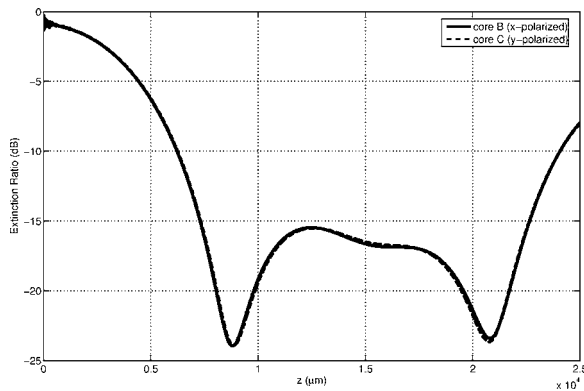Fig. 4.   Dominant magnetic field component of the y-polarized field after a 15.7 mm propagation in the device.

Fig. 5. Extinction ratios for the x and y polarizations as a function of the splitter length z.

tures are evident in Figs. 3 and 4, which depict the field distribution of the main magnetic field components at a distance $z = 15.7$ mm for both input polarizations, clearly showing the displacement of the input field into the proper output core. It should be noted that the beam propagation method employed is based on the magnetic field; thus the x-polarized mode exhibits H_y as the dominant magnetic component, while H_x is dominant for the y-polarized mode.

The power curves depicted in Fig. 2 show maximum coupling for a device length of 15.7 mm; both extinction ratios assume a value of about −17 dB, as shown in Fig. 5, with excellent performance matching. Beyond this length the field starts to couple back into the input core, but when the length is increased to 20.75 mm the extinction ratio for both cores reaches a minimum value of −23.5 dB. In this case the power exchange is lower, but the coupling ratio is still satisfactory, being slightly higher than 70%. Another extinction ratio minimum exists at a shorter length, but with an unsatisfactorily low coupled power. It is finally important to note that these good results hold over a wide wavelength range, as the extinction ratios remain below −22 dB over a 40 nm range and below −20 dB over a 90 nm range, both centered at $\lambda = 1.5 \ \mu$m.

A new polarization splitter based on a three-core square-lattice photonic-crystal fiber has been designed. The small size of the proposed device leads to high performance and overcomes the limits shown by previous designs based on triangular-lattice PCFs. A large spacing is obtained between the output cores, permitting easier connection to the external output ports. The twofold symmetry of the square lattice has been exploited to obtain excellent matching of the device's behavior with respect to the two orthogonal polarizations. The effect of hole perturbations introduced during fabrication will be the object of future work.

L. Rosa's e-mail address is lrosa@ieee.org.

References

1. T. Hayakawa, S. Asakawa, and Y. Kokubun, J. Lightwave Technol. **15**, 1165 (1997).
2. L. Soldano, A. H. de Vreede, M. K. Smit, B. H. Verbeek, E. G. Metaal, and F. H. Groen, IEEE Photon. Technol. Lett. **6**, 402 (1994).
3. K. Lin, W. Chaung, and W. Lee, J. Lightwave Technol. **14**, 2547 (1996).
4. L. Zhang and C. Yang, J. Lightwave Technol. **22**, 1367 (2004).
5. L. Zhang and C. Yang, IEEE Photon. Technol. Lett. **16**, 1670 (2004).
6. K. Saitoh, Y. Sato, and M. Koshiba, Opt. Express **12**, 3940 (2004).
7. S. Selleri, L. Rosa, F. Poli, and A. Cucinotta, in *Lasers and Electro-Optical Society 2004* (IEEE-LEOS, 2004), p. 647.
8. A. H. Bouk, A. Cucinotta, F. Poli, and S. Selleri, Opt. Express **12**, 941 (2004).
9. Y. C. Liu and Y. Lai, Opt. Express **13**, 225 (2005).
10. F. Poli, M. Foroni, M. Bottacini, M. Fuochi, N. Burani, L. Rosa, A. Cucinotta, and S. Selleri, J. Opt. Soc. Am. A **22**, 1655 (2005).
11. J. Y. Y. Leong, S. Asimakis, F. Poletti, P. Petropoulos, X. Feng, R. C. Moore, K. E. Frampton, T. M. Monro, H. Ebendorff-Heidepriem, W. H. Loh, and D. J. Richardson, in *ECOC-2005 31st European Conference on Optical Communication* (IEEE, 2005), paper Th 4.4.5.